ORIGINAL ARTICLE

Severe Pneumococcal Pneumonia Causes Acute Cardiac Toxicity and Subsequent Cardiac Remodeling

Luis F. Reyes[1,2]*, Marcos I. Restrepo[1,2]*, Cecilia A. Hinojosa[1,2], Nilam J. Soni[1,2], Antonio Anzueto[1,2], Bettina L. Babu[1,2], Norberto Gonzalez-Juarbe[3], Alejandro H. Rodriguez[4,5], Alejandro Jimenez[6], James D. Chalmers[7], Stefano Aliberti[8,9,10], Oriol Sibila[11], Vicki T. Winter[12], Jacqueline J. Coalson[12], Luis D. Giavedoni[13], Charles S. Dela Cruz[14], Grant W. Waterer[15], Martin Witzenrath[16,17], Norbert Suttorp[16,17], Peter H. Dube[18], and Carlos J. Orihuela[3]

[1]Division of Pulmonary Diseases and Critical Care Medicine, [12]Department of Pathology, and [18]Department of Immunology and Microbiology, The University of Texas Health Science Center at San Antonio, San Antonio, Texas; [2]Division of Pulmonary Diseases and Critical Care Medicine, South Texas Veterans Health Care System, San Antonio, Texas; [3]Department of Microbiology, The University of Alabama at Birmingham School of Medicine, Birmingham, Alabama; [4]Critical Care Medicine, Hospital Universitari de Tarragona Joan XXIII, Rovira i Virgili University, Tarragona, Spain; [5]Biomedical Research Networking Center on Respiratory Diseases (CIBERES), Tarragona, Spain; [6]Cardiovascular Medicine, Heart & Vascular Institute, Cleveland Clinic, Abu Dhabi, United Arab Emirates; [7]School of Medicine, University of Dundee, Dundee, United Kingdom; [8]Department of Pathophysiology and Transplantation, University of Milan, Milan, Italy; [9]Cardio-thoracic Unit and Adult Cystic Fibrosis Centre, Milan, Italy; [10]Istituti di Ricovero e Cura a Carattere Scientifico, Granada Ospedale Maggiore Policlinico, Milan, Italy; [11]Division of Pulmonary Diseases, Department of Medicine, Hospital de la Santa Creu i Sant Pau, Autonomous University of Barcelona, Barcelona, Spain; [13]Texas Biomedical Research Institute, San Antonio, Texas; [14]Division of Pulmonary and Critical Care Medicine, Yale University, New Haven, Connecticut; [15]Royal Perth Hospital Unit, University of Western Australia, Perth, Australia; and [16]Department of Infectious Diseases and Pulmonary Medicine and [17]SFB-TR84 "Innate Immunity of the Lung," Charité-Universitätsmedizin Berlin, Berlin, Germany

ORCID IDs: 0000-0003-1172-6539 (L.F.R.); 0000-0001-9107-3405 (M.I.R.).

Abstract

Rationale: Up to one-third of patients hospitalized with pneumococcal pneumonia experience major adverse cardiac events (MACE) during or after pneumonia. In mice, *Streptococcus pneumoniae* can invade the myocardium, induce cardiomyocyte death, and disrupt cardiac function following bacteremia, but it is unknown whether the same occurs in humans with severe pneumonia.

Objectives: We sought to determine whether *S. pneumoniae* can (*1*) translocate the heart, (*2*) induce cardiomyocyte death, (*3*) cause MACE, and (*4*) induce cardiac scar formation after antibiotic treatment during severe pneumonia using a nonhuman primate (NHP) model.

Methods: We examined cardiac tissue from six adult NHPs with severe pneumococcal pneumonia and three uninfected control animals. Three animals were rescued with antibiotics (convalescent animals). Electrocardiographic, echocardiographic, and serum biomarkers of cardiac damage were measured (troponin T, N-terminal pro-brain natriuretic peptide, and heart-type fatty acid binding protein). Histological examination included hematoxylin and eosin staining, immunofluorescence, immunohistochemistry, picrosirius red staining, and transmission electron microscopy. Immunoblots were used to assess the underlying mechanisms.

Measurements and Main Results: Nonspecific ischemic alterations were detected by electrocardiography and echocardiography. Serum levels of troponin T and heart-type fatty acid binding protein were increased ($P < 0.05$) after pneumococcal infection in both acutely ill and convalescent NHPs. *S. pneumoniae* was detected in the myocardium of all NHPs with acute severe pneumonia. Necroptosis and apoptosis were detected in the myocardium of both acutely ill and convalescent NHPs. Evidence of cardiac scar formation was observed only in convalescent animals by transmission electron microscopy and picrosirius red staining.

Conclusions: *S. pneumoniae* invades the myocardium and induces cardiac injury with necroptosis and apoptosis, followed by cardiac scarring after antibiotic therapy, in an NHP model of severe pneumonia.

Keywords: pneumococcal pneumonia; *Streptococcus pneumoniae*; cardiovascular complications; community-acquired pneumonia

At a Glance Commentary

Scientific Knowledge on the Subject: *Streptococcus pneumoniae* is the most frequently isolated bacterial pathogen in patients with community-acquired pneumonia (CAP). As a result of highly complex host–pathogen interactions, patients with pneumococcal pneumonia are at increased risk of developing cardiovascular complications during and after CAP, including heart failure, arrhythmias, stroke, and acute coronary syndrome. Recent studies in mice revealed that *S. pneumoniae* is capable of invading the heart and causing direct cardiac damage during invasive pneumococcal disease. Yet, murine pneumococcal pneumonia is poorly representative of human disease, and whether cardiac invasion occurs during severe pneumonia in humans is unknown. Our aim in this study was to determine, using a validated nonhuman primate model that closely resembles pneumococcal disease in humans, if pneumococcus (*1*) invades the myocardium, (*2*) induces cardiomyocyte death, and (*3*) elicits cardiovascular complications during pneumococcal pneumonia.

What This Study Adds to the Field: This study presents novel evidence that *S. pneumoniae* can invade the heart during severe pneumonia and induce cardiomyocyte death via direct cytotoxic effects. These findings could potentially explain the development of short- and long-term cardiac complications associated with CAP due to acute cardiomyocyte injury and induction of scar formation in the hearts of convalescent nonhuman primates.

Lower respiratory tract infections cost the healthcare system more than $10 billion annually in the United States (1, 2). Community-acquired pneumonia (CAP) and influenza infections together represent the fourth most prevalent cause of death worldwide (3). The morbidity, mortality, and costs associated with CAP have remained unchanged in recent decades, despite the availability of antibiotic treatments and preventive strategies with immunizations (4, 5). Approximately 30% of patients hospitalized with CAP experience major adverse cardiac events (MACE) during hospitalization and up to 10 years after infection (6–9). Importantly, patients with pneumonia and MACE have double the hospital mortality compared with those with pneumonia alone (6, 10). MACE in patients with CAP include new-onset or worsening heart failure, arrhythmias, stroke, and acute coronary syndrome (9). Risk factors for MACE during CAP include infection with *Streptococcus pneumoniae*, older age, severe CAP, hyperlipidemia, obesity, and arterial hypertension (6, 8, 11, 12). The pathophysiology of MACE during CAP has been attributed to the complex host–pathogen interactions, but the exact mechanisms are not well understood (9, 13).

S. pneumoniae (pneumococcus) is the most frequent bacterial pathogen in patients with CAP (14, 15). Pneumococcal pneumonia has been identified as an independent risk factor for the development of MACE during CAP (6, 8, 11, 12, 16). Pneumococcal pneumonia can result in cardiovascular complications in 10 to 30% of patients, affecting mainly those with existing cardiovascular diseases (11, 12). Recently, our research group (17, 18) and other researchers (19–21) have described that the pneumococcus and its virulence factors (e.g., pneumolysin, bacterial cell wall) have direct detrimental effects on the cardiac function of rodents with invasive pneumococcal disease (IPD). We have demonstrated that pneumococcus can invade the heart and cause small, bacteria-filled lesions within the myocardium (17, 18). These myocardial lesions disrupt cardiac contractility, induce cardiomyocyte death, and subsequently cause *de novo* collagen deposition in mice rescued with antibiotics (convalescent mice) (17, 22). Moreover, we have shown that *S. pneumoniae* is capable of inducing necroptosis, a highly proinflammatory programmed cell death pathway, in lung macrophages during pneumonia (23). Pertinent to the present study, necroptosis has been recognized as a key cell death pathway in cardiomyocytes during ischemia-reperfusion injury and acute coronary syndrome (24–26).

Despite epidemiological studies demonstrating that pneumococcal infection is an independent risk factor for MACE (6–8, 11, 12), it is unknown whether *S. pneumoniae* can generate direct cardiac cytotoxicity (e.g., cell death), heart failure, clinically relevant arrhythmias, or acute coronary syndrome (i.e., MACE) in humans with severe pneumococcal pneumonia (11, 12, 16, 27). Additionally, the potential underlying mechanisms of MACE during pneumococcal pneumonia have been described in rodent models, but it is speculative to extrapolate these findings to humans. To address this knowledge gap, we used a validated nonhuman primate (NHP) model of severe pneumococcal pneumonia that closely mimics human disease (28) to explore the mechanisms of pneumococcal cytotoxicity on cardiomyocytes. Potential translation of these findings to humans includes identification of potential therapeutic targets to prevent MACE and, ultimately, improvement in clinical outcomes of patients with CAP.

Methods

These animal studies were performed at the Texas Biomedical Research Institute in San Antonio, Texas. This animal protocol along with all animal experiments were reviewed and approved by the institutional animal care and use committee (IACUC number 1443PC6) at the Texas Biomedical Research Institute.

Study Design

A full description of the NHP model of severe pneumococcal pneumonia has been published previously (28). Briefly, six healthy adult baboons (*Papio cynocephalus*), including four males, were bronchoscopically challenged with 10^9 colony-forming units of *S. pneumoniae* serotype 4 (strain TIGR4 [29]). Collection of blood for serum biomarkers and bacterial load estimation, acquisition of a 12-lead ECG and a transthoracic echocardiogram, and bronchoalveolar lavage were performed before the infection and at the end of the experiment before animals were killed (28). Continuous 24-hour temperature, heart rate, and three-lead ECG were recorded throughout the experiment via a surgically implanted tether. At the end of the experiment, the hearts were harvested and prepared for tissue experiments. Three NHPs were treated with intravenous ampicillin (80 mg/kg/d) for 7 days (the convalescent group) (28). All ECGs were read by an expert electrophysiologist (A.J.) who was blinded to the experiment results. The study design is summarized in Figure E1 in the online supplement. Finally, MACE were defined as heart failure, arrhythmias, or myocardial infarctions.

Study Groups

The cohort was divided in two groups to mimic the preantibiotic era and modern era of patients with pneumonia (28). For the preantibiotic era group, we did not treat three NHPs with antibiotics, and they were called the *acute pneumonia group* and killed per protocol 4–6 days after infection. In the modern era of pneumonia group, three NHPs were rescued with antibiotic treatment, and they were called the *convalescent pneumonia group* and killed per protocol 9–14 days after infection (28). The end of the experiment refers to the moment before animals were killed, which varied for each animal

according to the study groups just described (28). Heart tissues of three age- and sex-matched uninfected NHPs served as controls (Figure E1).

Transthoracic Echocardiogram Evaluation

A standard five-view focused cardiac ultrasound examination was performed using a portable ultrasound machine (GE LOGIQ e Vet; GE Healthcare, Little Chalfont, UK) equipped with microconvex (GE model 8C-RS, 4.0–10.0 MHz; GE Healthcare) and phased-array (GE model 3S-RS, 1.7–4.0 MHz; GE Healthcare) transducers. Parasternal long- and short-axis, apical and subcostal four-chamber, and subcostal inferior vena cava (IVC) views were obtained to assess the left ventricular (LV) and right ventricular size and function, cardiac valves, pericardium, and IVC size and collapsibility.

Serum Cardiac Biomarkers

Serum levels of ultrasensitive troponin T (Life Diagnostics, West Chester, PA), heart-type fatty acid binding protein (H-FABP; Kamiya Biomedical, Seattle, WA), and N-terminal pro-brain natriuretic peptide (Neo Scientific, Cambridge, MA) were measured by ELISA in serum samples before infection and at the end of the experiment. Cytokine and chemokine analyses were performed using a validated Luminex multiplex assay for NHPs (30).

Tissue Staining and Microscopy

Immunofluorescent and immunohistochemical (IHC) staining was performed with paraffin-embedded tissues as previously described (18). Primary antibodies used in this study included those against serotype 4 capsular polysaccharide antibody (Statens Serum Institut,

Copenhagen, Denmark); pneumolysin (Santa Cruz Biotechnology, Dallas, TX), transforming growth factor (TGF)-β (Bio-Rad Laboratories, Hercules, CA), pSMAD3, mixed lineage kinase domain-like pseudokinase (MLKL), phosphorylated MLKL (pMLKL), caspase 3 (Cell Signaling Technology, Danvers, MA), receptor-interacting protein kinase 3 (RIP3; Abcam, Cambridge, UK), and hypoxia-inducible factor (HIF)-1α (Bethyl Laboratories, Montgomery, TX). The secondary antibody used was fluorescein isothiocyanate–labeled goat antirabbit antibody (Jackson ImmunoResearch, West Grove, PA). Picrosirius red–stained (Electron Microscopy Sciences, Hatfield, PA) and hematoxylin and eosin–stained heart sections were scanned with an Aperio ScanScope XT scanner (Aperio Technologies, Leica Biosystems, Wetzlar, Germany). Immunofluorescent and IHC images were captured with an Olympus AX70 microscope (Olympus America, Center Valley, PA). Transmission electron microscopy (TEM) was performed with a JEOL JEM 1230 transmission electron microscope (JEOL, Peabody, MA).

Immunoblotting

Hearts were homogenized and processed as previously described (23) with protease (Sigma-Aldrich, St. Louis, MO) and phosphatase (Thermo Fisher Scientific, Waltham, MA) inhibitors.

Statistical Analysis

All data are presented as median with interquartile range (IQR) or mean with SD as appropriate. Paired nonparametric Wilcoxon signed-rank tests or two-tailed Student's *t* tests were used to compare data at different time points. All statistical

Table 1. Twelve-Lead ECG Quantitative Analysis of All Six Nonhuman Primates

Variable	Baseline	End of Experiment	P Value
Heart rate, beats/min	78 (69–99.5)	122 (102.5–152)	**0.001**
P-wave duration, ms	80 (76.5–87.5)	80 (70–100)	0.728
PR interval, ms	140 (121.5–155)	135 (125–155)	0.893
RR interval, ms	769.23 (603.15–869.74)	491.93 (394.73–586.36)	**0.001**
QRS interval, ms	55 (47.5–62.5)	55 (50–63.75)	0.874
QT interval, ms	310 (287.5–347.5)	292.50 (281.25–317.5)	0.323
Corrected QT interval, ms	369.76 (341.53–398.36)	440.20 (398.29–454.36)	**0.001**
ST segment, ms	125 (100–160)	114 (91.25–132.5)	0.308
T-wave duration, ms	125 (120–140)	130 (125–143.75)	0.229

Data are presented as median with interquartile range, and statistically significant *P* values are presented in bold.

calculations were performed using Prism 5 software (GraphPad Software, La Jolla, CA). Two-tailed *P* values less than 0.05 were considered statistically significant.

Results

Six NHPs with a median age of 11 (IQR, 10–19) years, which corresponds to middle-aged to elderly in humans, were included in the study. Details about each NHP, as well as an overview of the experiments done to develop the severe pneumococcal pneumonia model, were previously described (28). Demographics and pneumonia severity are presented in Table E1.

Noninvasive Cardiac Evaluation

ECG evaluation. During baseline evaluation, all animals were in sinus rhythm with normal PR, QT, and ST intervals (Table 1, Figure 1A). P, T, and QRS waves resembled their normal morphology in humans (Figure 1A). At the end of the experiment, immediately before the animals were killed, ECG evaluation showed that all six NHPs had developed sinus tachycardia, diffuse repolarization abnormalities represented by diffuse ST segment changes, T-wave flattening, and prolongation of the corrected QT interval (Figures 1B–1E, Table 1). Table 2 presents the individual interpretations of the 12-lead ECGs at baseline and at the end of the experiment. No other significant alterations were detected in the ECG tracings, even after the cohort was stratified by acute or convalescent pneumonia (Table E2).

Echocardiographic findings. A qualitative focused cardiac ultrasound examination was conducted at baseline and at the end of the experiment. Findings are summarized in Table E3. Prior to infection, all six NHPs had normal focused cardiac ultrasound examinations. NHPs with acute pneumonia demonstrated hyperdynamic LV function, moderate tricuspid regurgitation, small pericardial effusions, and collapsed IVCs (central venous pressure <5 mm Hg). NHPs with convalescent pneumonia developed increased LV relative wall thickness and some associated wall motion abnormalities (hypokinesis).

Serum biomarkers. Troponin T and H-FABP serum levels were elevated at the end of the experiment in all NHPs compared with baseline levels (median [IQR], 0.005 ng/ml [0.000–0.025] vs. 0.044 ng/ml
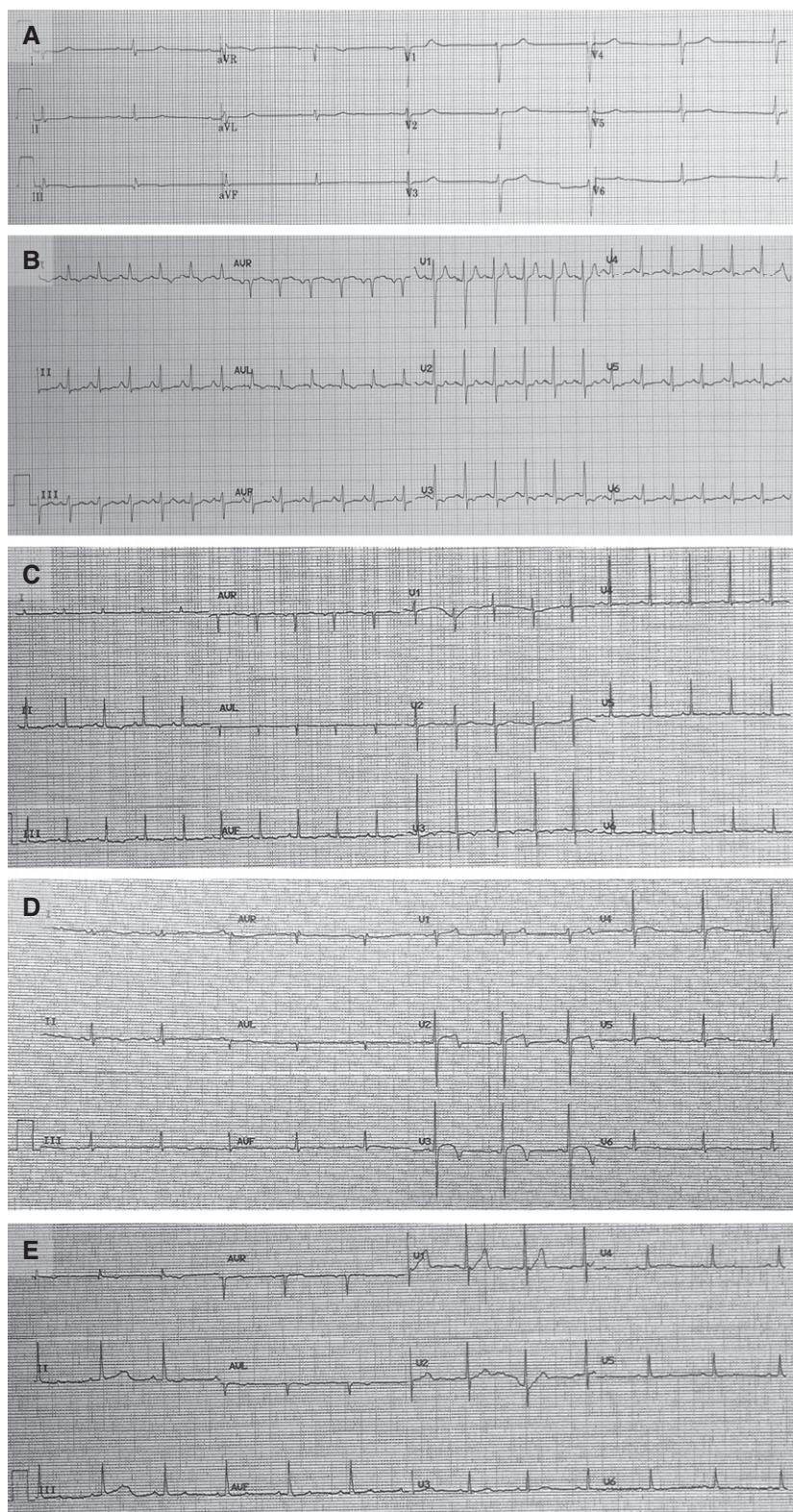
Figure 1. Nonhuman primates with severe pneumococcal pneumonia developed diffuse, nonspecific repolarization abnormalities. Twelve-lead ECGs were recorded (*A*) at baseline and (*B–E*) at the end of the experiment. (*A*) At baseline, all animals were in sinus rhythm with no repolarization abnormalities. After development of pneumococcal pneumonia, the ECGs consistently showed (*B* and *C*) sinus tachycardia and (*B–E*) abnormal repolarization (i.e., diffuse T-wave and ST-segment flattening).

Table 2. Qualitative Individual Interpretation of 12-Lead ECGs at Baseline and End of the Experiment

	Animal	Electrocardiographic Findings	
		Baseline	End of Experiment
Acute pneumonia	1	Biphasic T waves in lateral leads	Inverted T waves in inferior and anterolateral leads
	2	No repolarization abnormalities	Slow ventricular rhythm
	3	Diffuse ST-segment and T-wave flattening	Q waves on lateral leads, ST-segment and T-wave flattening in inferolateral leads
Convalescent pneumonia	4	No repolarization abnormalities	Diffuse ST-segment and T-wave flattening
	5	Short QT segment	Diffuse ST-segment and T-wave flattening
	6	No repolarization abnormalities	Q waves in lateral leads, T-wave inversion in lateral leads, and ST-segment depression in inferior leads

[0.036–0.057]; $P = 0.002$; and 150.8 ng/ml [33.25–281.5] vs. 916.9 ng/ml [595.8–1,323]; $P = 0.002$, respectively) (Figures 2A and 2C). When we stratified the cohort by acute or convalescent pneumonia (i.e., with vs. without antibiotic treatment), troponin T and H-FABP remained higher at the end of the experiment in both cohorts, but the troponin T concentration was not statistically significant higher than it was at baseline (Figures 2B and 2D). In contrast,
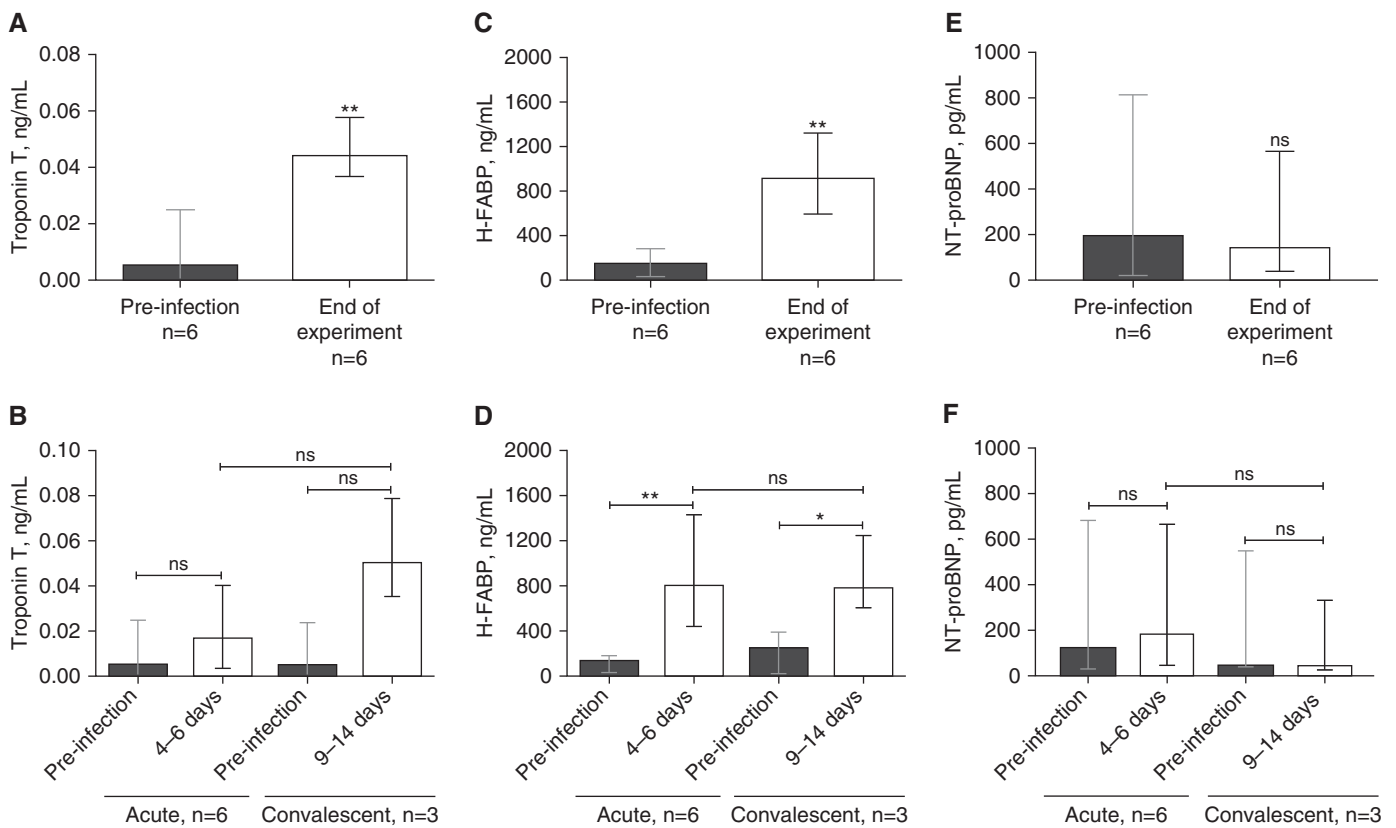
Figure 2. Serum concentrations of cardiac damage biomarkers were elevated in animals with acute and convalescent pneumococcal pneumonia. The serum biomarkers of cardiac damage, troponin T, heart-type fatty acid binding protein (H-FABP), and N-terminal pro-brain natriuretic peptide (NT-proBNP) were assessed before infection, at Days 4–6 for the acute group, and at Days 9–14 for the convalescent group. Median ($n = 6$) serum concentrations of (*A*) troponin T, (*C*) H-FABP, and (*E*) NT-proBNP are shown before infection and at the end of the experiment (i.e., before animals were killed). To test whether antibiotic treatment could prevent cardiac damage, the cohort was stratified into nonhuman primates with acute pneumonia (i.e., without antibiotics; $n = 6$) and nonhuman primates with convalescent pneumonia (i.e., with antibiotics; $n = 3$). Serum levels of (*B*) troponin T, (*D*) H-FABP, and (*F*) NT-proBNP were assessed for each group before infection, at Days 4–6 for the acute group, and at Days 9–14 for the convalescent group. Values are shown as medians with interquartile ranges. A paired nonparametric Wilcoxon signed-rank test was used to analyze statistical differences among the groups. *$P < 0.05$; **$P < 0.01$. ns = not significant.

serum N-terminal pro-brain natriuretic peptide serum levels did not change significantly at the end of the experiment (194.2 pg/ml [22.21–815.1] vs. 141.9 pg/ml [39.8–565.5]; $P = 0.9$) (Figures 2E and 2F).

Invasive Cardiac Evaluation

***Detection of* S. pneumoniae.** We performed immunofluorescent staining of the different parts of the heart in all animals and confirmed the invasion of *S. pneumoniae* in the myocardium (Figure 3A and 3B). In NHPs with acute pneumonia, we observed clusters of pneumococci, suggesting that the bacteria were capable of replicating within the tissue. In contrast, in NHPs with convalescent pneumonia, only a few punctate points were observed, representing *S. pneumoniae* capsule debris (Figure 3C). Quantification of bacteria in heart homogenates confirmed that *S. pneumoniae* was present in NHPs with acute pneumonia, and none was detected in those with convalescent pneumonia or in uninfected control animals (Figure E2).

Histopathological findings. Tissue sections of the right or left ventricle and the interventricular septum showed similar lesions of a focal cardiac injury, primarily in perivascular sites, of varying extent and severity determined by hematoxylin and eosin staining (Figure E3). Affected cardiac

myocytes were enlarged, with a striking increase in eosinophilic staining, and were well demarcated from adjacent cardiac tissue (Figures 4A–4C). The damage of left ventricles and septum varied in terms of size and infiltration (Figure E3). Varying degenerative and/or necrotic lesions were observed in the left ventricle and interventricular septum (Figures 4A–4C). All animals had mild to severe myocyte fatty change and vacuolization, focal contraction bands, interstitial edema, focal myocytolysis, and scattered inflammatory cells (Figures 4A and 4B). We observed scattered myocytolysis in several myocytes (Figures 4A and 4B), but prominent nuclear pyknosis with extensive myocytolysis was apparent in several myocytes (Figure 4C). Two NHPs exhibited additional necrotic lesions defined by nuclear karyolysis and fragmentation, although one site had some clumped bacteria (Figure 4C).

Using TEM, we observed that infected NHPs consistently developed areas of vacuolization with focal contraction bands and interstitial edema in the left ventricle and septum (Figures 4E and 4F). Additionally, we identified several areas with focal myocytolysis and nuclear pyknosis that corresponded to extensive mitochondrial damage characterized by swollen and electron-lucent matrices (Figure 4G). Moreover, the mitochondrial

cristae were degraded and disorganized and had decreased density. All these changes were evident in both the acute and convalescent pneumonia groups (Figures 4E–4G).

Cardiac inflammatory response. We observed high concentrations of cytokines and chemokines, including IL-6, tumor necrosis factor (TNF)-α, IL-8, IL-1β, IL-1Rα, and macrophage inflammatory protein 1α in homogenized hearts (left ventricle and interventricular septum) of all NHPs with acute pneumonia (Figure 5). All three NHPs with convalescent pneumonia had lower heart concentrations of cytokines and chemokines than NHPs with acute pneumonia (Figures 5A–5F). Significantly higher concentrations of IL-6, TNF-α, and IL-1β were seen in the left ventricle and interventricular septum of infected NHPs versus uninfected control animals (Figures 5B, 5D, and 5E). IL-8 levels were higher in the interventricular septum (Figure 5C) of NHPs with convalescent pneumonia than in uninfected control animals.

Cardiomyocyte death. To test the role of necroptosis in cardiomyocyte death, we stained for RIP3 and pMLKL (necroptosis effector) in heart tissues from infected NHPs with acute and convalescent pneumonia and uninfected control animals using IHC staining (Figure 6A). An increased signal of both RIP3 and pMLKL was seen in stained tissues, suggesting that necroptosis was taking place throughout the myocardium. Increased levels of both RIP3 and pMLKL were confirmed by immunoblot analysis (Figure 6B). Additional staining of cardiac tissues with CardioTAC (R&D Systems, Minneapolis, MN) suggested apoptotic cells in the myocardium (Figure E4). Briefly, CardioTAC labels DNA ends using terminal deoxynucleotidyl transferase. In addition, consistent with the presence of apoptotic cells in the myocardium, we observed an increase of apoptosis effector caspase 3 mainly in NHPs with acute pneumonia (Figure E4). Collectively, these results suggest that *S. pneumoniae* induces programmed death pathways after it invades the myocardium.

Cardiac fibrosis. TGF-β in the heart stimulates myofibroblasts to produce collagen to replace dead cardiomyocytes (31, 32). After *S. pneumoniae* had induced necroptosis in the heart, *de novo* collagen deposition was detected in the left ventricle and septum, as evidenced by picrosirius red staining (Figure 7A) and TEM (Figure 7B). Collagen deposition was seen 9–14 days

4C/FPO

■ DAPI ■ Capsule *Streptococcus pneumoniae*
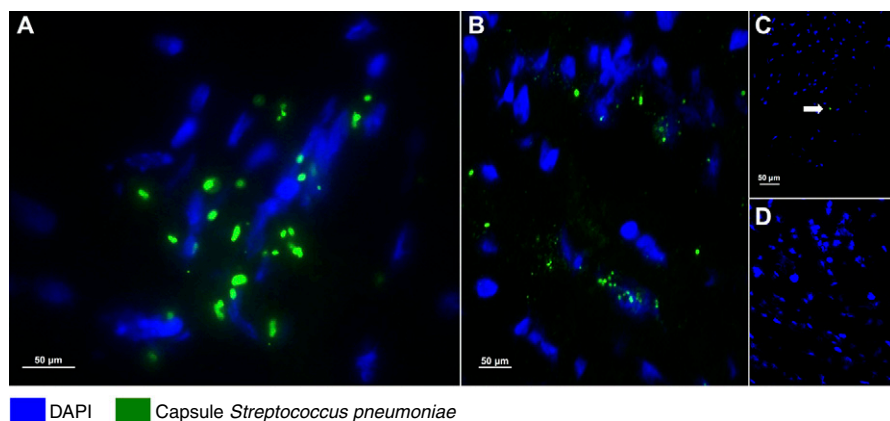
Figure 3. *Streptococcus pneumoniae* translocates into the heart during pneumonia. Representative images from (*A* and *C*) left ventricular and (*B*) interventricular septal sections from the six nonhuman primates (NHPs) with pneumococcal pneumonia and (*D*) three uninfected control animals. *S. pneumoniae* was visualized using immunofluorescent staining with antiserum against serotype 4 capsular polysaccharide (*green*) and 4′,6-diamidino-2-phenylindole (DAPI; *blue*) to reveal nucleated tissue cells. (*A* and *B*) Bacterial aggregates with diplococci morphology are seen within the left ventricles and septa of NHPs with acute pneumonia. (*A*) Bacterial cluster conformation indicates active replication. (*C*) Single-capsule debris (marked with the *white arrow*) were scattered throughout the left ventricles and in the interventricular septa of convalescent NHPs. (*D*) Pneumococcal capsules were not identified in the hearts of uninfected control NHPs.

4C/FPO
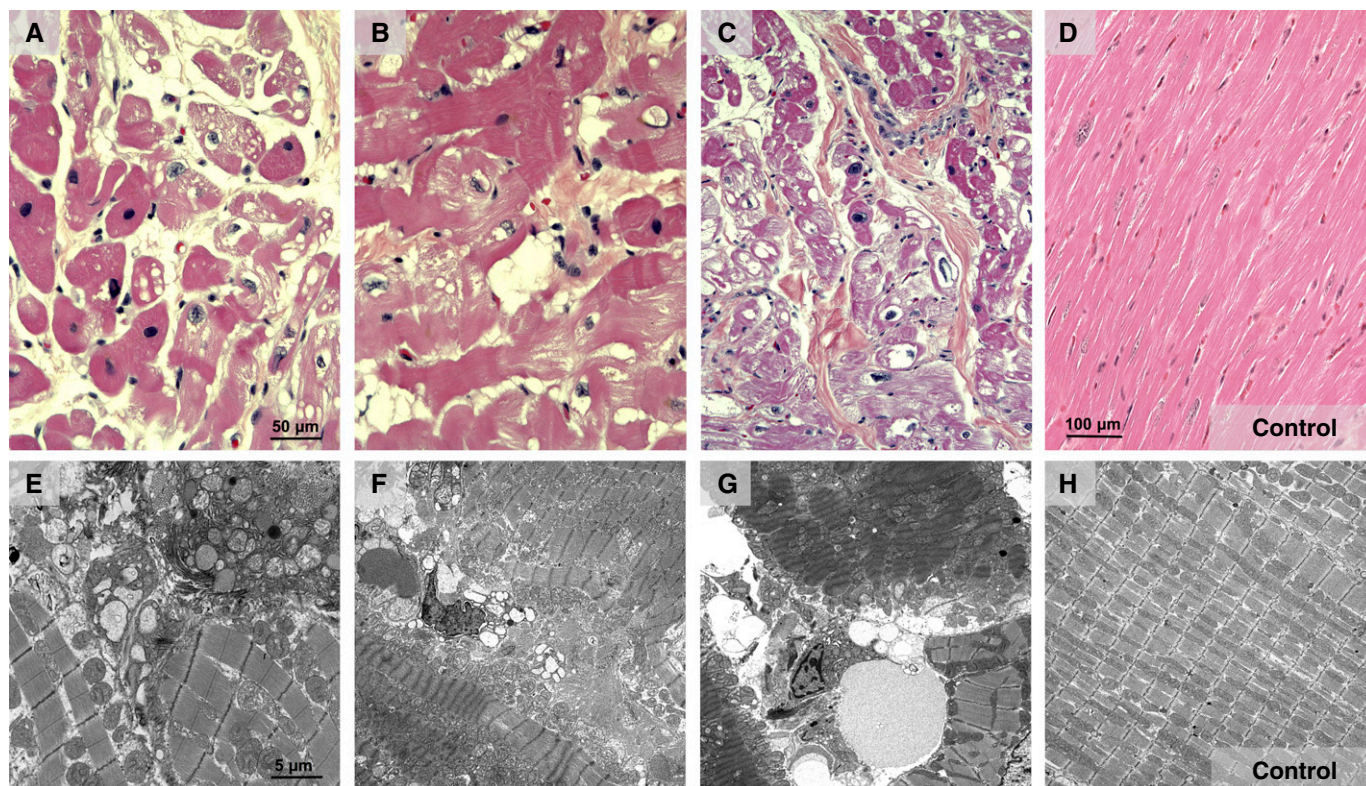
Figure 4. Hearts of nonhuman primates (NHPs) with severe pneumonia developed severe cardiac injury with variable pathological characteristics. Representative hematoxylin and eosin–stained and transmission electron microscopic images of heart specimens from (*A*, *B*, and *E*) NHPs with acute pneumococcal pneumonia and (*C*, *F*, and *G*) NHPs with convalescent pneumonia, as well as (*D* and *H*) uninfected control NHPs. (*A* and *G*) NHPs developed myocyte cytoplasm degenerative changes, including fatty change, vacuolization, and myofibrillar separation. (*A* and *E*) Perinuclear and interstitial edema are evident, and several myocyte nuclei contain condensed chromatin, a necrotic change. (*B* and *F*) Additionally, in the left ventricle, myocytes with cytoplasmic changes of contraction bands, focal vacuolization, and myocytolysis were identified. (*B*) The edematous interstitium contained increased small mononuclear cells and some neutrophils. (*B* and *G*) Nuclear edema and karyolysis are diffusely evident in cardiomyocytes. (*C*, *E*, and *F*) Widespread myocytolysis, contraction bands, striking nuclear pyknosis, and karyolysis are seen in the septum. (*F* and *G*) Finally, degradation of mitochondrial cristae and edema were consistently observed by transmission electron microscopy.

after infection in convalescent animals. Additionally, using immunoblot analysis, we identified increased expression of pSMAD3, which stimulates collagen production in cardiac myofibroblasts (33).

Finally, to confirm that cardiac injury and collagen deposition were secondary to *S. pneumoniae* invasion, we explored the HIF-1α pathway that is activated by hypoxia (34). Immunoblotting in homogenized hearts of NHPs confirmed that the HIF-1α pathway was downregulated in both the acute and convalescent pneumonia groups (Figure E5).

Discussion

The results of our study provide novel evidence that, similarly to humans, NHPs with severe pneumococcal pneumonia

develop signs of cardiac injury, including diffuse repolarization abnormalities, hyperdynamic LV function, and mild elevation of serum biomarkers (i.e., troponin T and H-FABP). Microscopic examination of heart tissues revealed that pneumococcus is capable of translocating into the myocardium and inducing cardiomyocytes by necroptosis and apoptosis. Moreover, we confirmed that heart invasion by *S. pneumoniae* causes severe cardiac injury and local proinflammatory responses independent of antibiotic treatment. We provide evidence that NHPs with convalescent pneumonia develop interstitial collagen deposition (i.e., scar formation) secondary to TGF-β pathway activation. Our findings are novel in that they provide translational data highlighting the etiological role of *S. pneumoniae* in causing MACE in

patients with pneumonia. Further, collagen deposition in the myocardium may explain the increased long-term risk of MACE after an acute episode of pneumococcal pneumonia.

Up to 36% of patients hospitalized with CAP develop severe disease, which requires admission to the intensive care unit (35, 36). Owing to the severe inflammatory response and mitochondrial dysfunction during severe pneumonia, at least 30% of patients develop LV dilation with a reduced ejection fraction, which usually takes 7–10 days to recover (i.e., sepsis-induced cardiomyopathy) (37, 38). In addition, Corrales-Medina and colleagues showed recently in a cohort study that 10 to 30% of adults (without a clinical history of cardiac disease) admitted for CAP developed clinically relevant heart failure, arrhythmias, or acute coronary syndrome
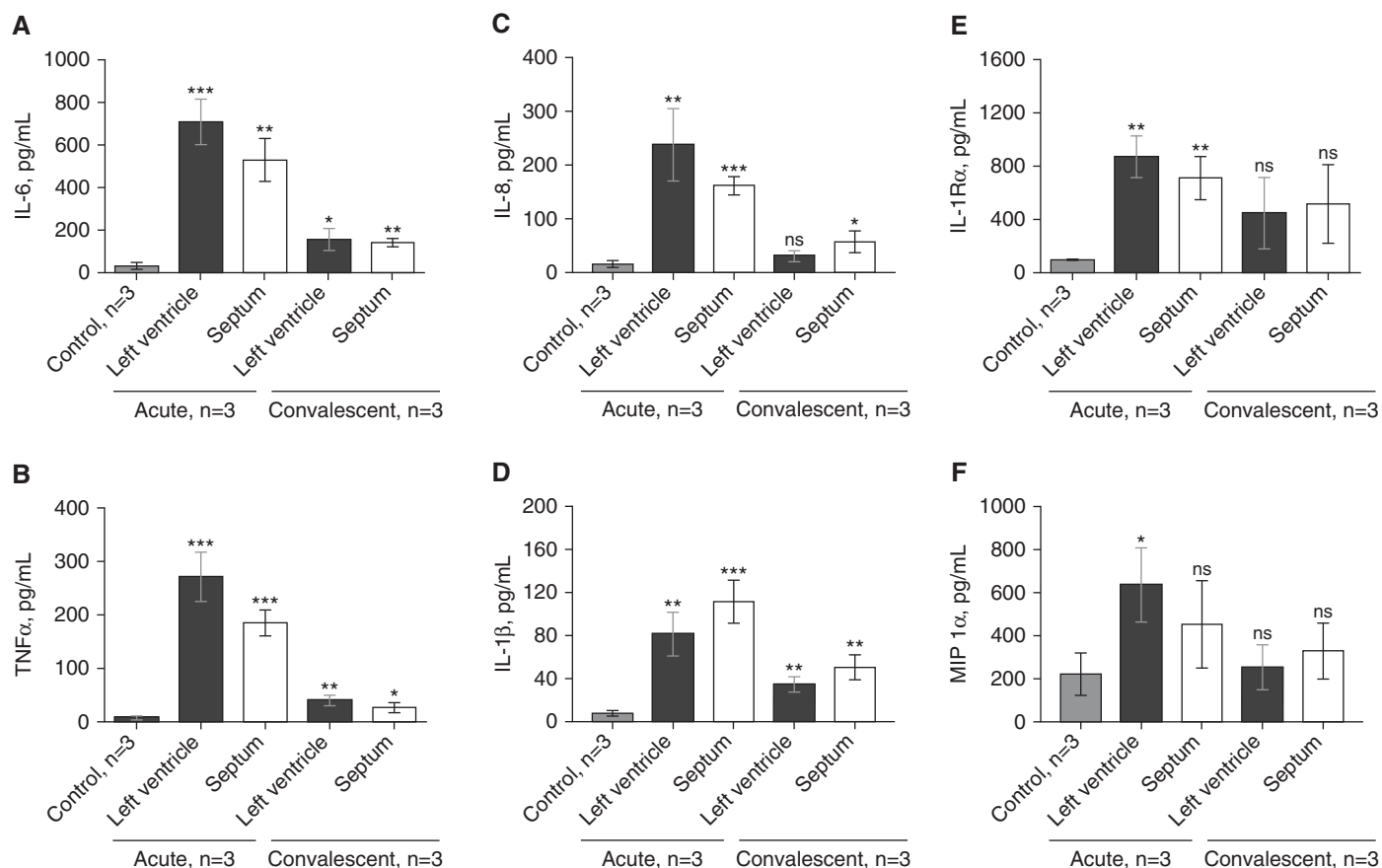
Figure 5. Cytokines and chemokines present in homogenized hearts of nonhuman primates (NHPs) with acute or convalescent pneumococcal pneumonia. Median concentrations of proinflammatory cytokines in homogenized left ventricles and interventricular septa of NHPs with acute and convalescent pneumococcal pneumonia are shown. NHPs with acute pneumonia had higher concentrations of (A) IL-6, (B) tumor necrosis factor (TNF)-α, (C) IL-8, (D) IL-1β, (E) IL-1Rα, and (F) macrophage inflammatory protein (MIP)-1α than uninfected NHPs. Convalescent NHPs had lower concentrations of cytokines than NHPs with acute pneumonia, but (A) IL-6, (B) TNF-α, (C) IL-8, and (D) IL-1β persisted at higher levels than in uninfected control animals. Values are shown as medians and interquartile ranges. An unpaired nonparametric Mann-Whitney U test was used to analyze statistical differences among the groups. All comparisons were made against uninfected control animals. *$P < 0.05$; **$P < 0.01$; ***$P < 0.001$. ns = not significant.

up to 10 years after hospitalization (6–8). More commonly, up to 59% of patients admitted with sepsis develop a cardiac phenomenon called *demand ischemia* (i.e., mild troponin elevation and repolarization abnormalities in the absence of myocardial infarction or coronary disease) rather than sepsis-induced cardiomyopathy or MACE (39–41). In our study, we found that all six previously healthy NHPs with pneumococcal pneumonia developed nonspecific cardiac changes that cannot be categorized as MACE but are consistent with what clinicians call *demand ischemia*. In contrast to human studies, in our present study, we were able to perform a detailed *ex vivo* examination of the NHP hearts, which revealed that *S. pneumoniae* can invade the heart and induce severe cardiac injury by

killing cardiomyocytes through necroptosis and apoptosis.

S. pneumoniae and its virulence factors (e.g., pneumolysin, cell wall) are cytotoxic and capable of inducing inflammation in cardiomyocytes (17, 19, 20). Recently, our research group described the novel observation that the pneumococcus is capable of invading the myocardium and forming nonpurulent, bacteria-filled, microscopic lesions that were associated with cardiomyocyte death (apoptosis) and electrocardiographic abnormalities in mice with IPD (22). In our experiments with severe pneumococcal pneumonia in NHPs, we proved that the pneumococcus is capable of invading the bloodstream and translocating the myocardium. In the hearts of NHPs, *S. pneumoniae* was observed in clusters, representing active replication,

which did not form microlesions as previously described in mice (18). This difference may be explained by the high bacterial load and longer infection times required to develop mature microlesions. Gilley and colleagues (18) recently described how cardiac invasion by pneumococcus occurs as soon as 12 hours after infection, but microlesion formation was dependent on bacterial load and time. Although similar findings have been reported in an IPD model that is not representative of pneumococcal pneumonia in humans, we used an NHP model of severe pneumonia that closely mimics the development and pathogenesis of human disease in that all the animals develop low-grade bacteremia for a short period (28).

Cardiomyocytes have been shown to die by apoptosis or necroptosis during
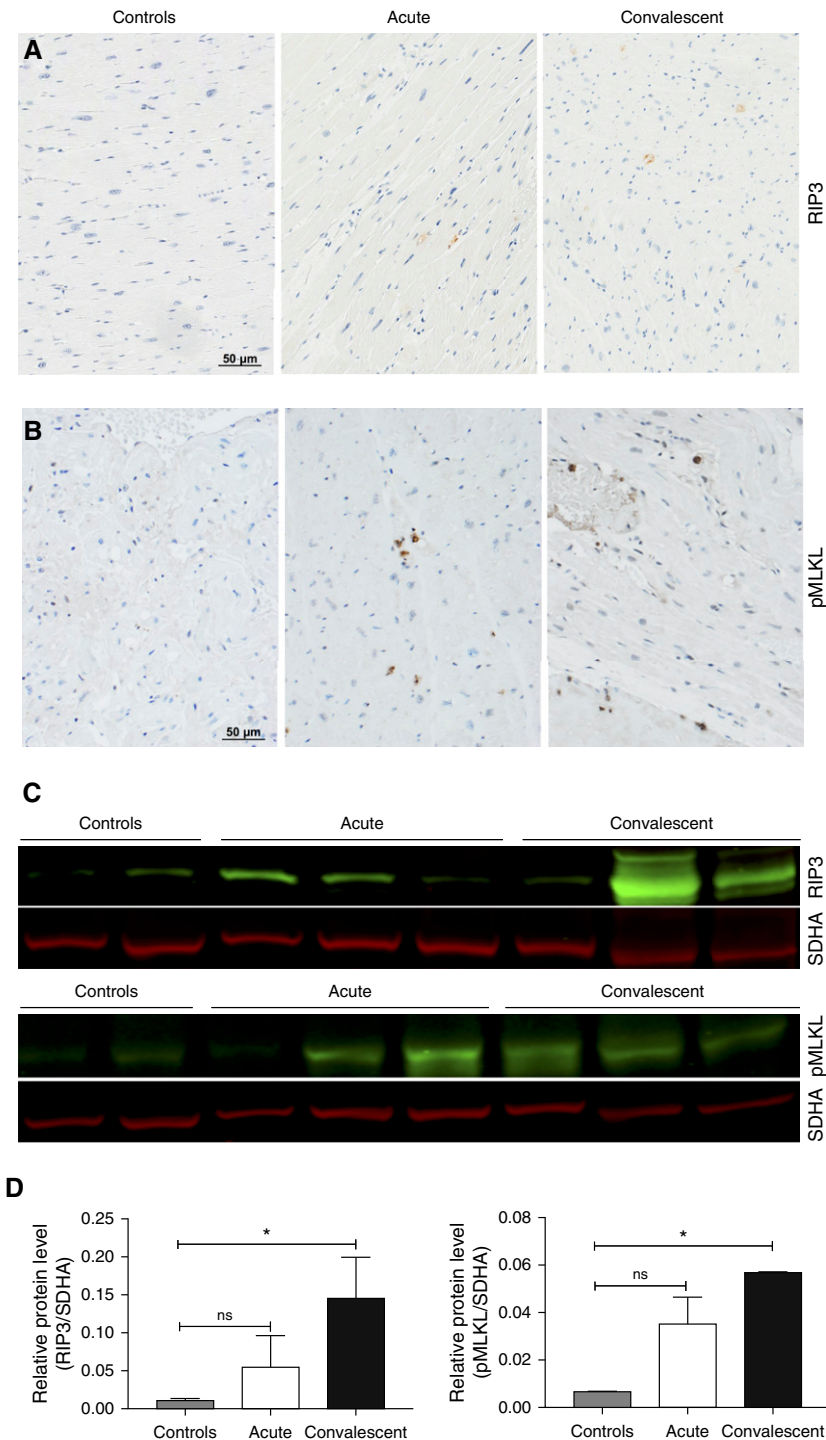
Figure 6. Necroptosis in heart tissue increases after antibiotic treatment. Immunohistochemistry was used to elucidate the cell pathways involved during cell death in nonhuman primates (NHPs) with pneumococcal pneumonia. Immunohistochemistry of heart sections stained for (*A*) receptor-interacting protein kinase 3 (RIP3) and (*B*) phosphorylated mixed lineage kinase domain-like pseudokinase (pMLKL). (*C*) Immunoblot analysis for RIP3, pMLKL, and succinate dehydrogenase complex, subunit A (SDHA; loading control), in heart tissue of infected NHPs versus uninfected control animals. (*D*) Relative levels of RIP3 and pMLKL protein expression determined by comparing the ratio of the detected band with total protein levels as determined using LI-COR Image Studio Lite software (LI-COR Biosciences, Lincoln, NE). Values are shown as medians and interquartile ranges. Unpaired nonparametric Mann-Whitney *U* tests were used to analyze statistical differences among the groups. *$P < 0.05$. ns = not significant.

injury or disease (24–26). Apoptosis is an immunoquiescent form of cell death that requires the activity of cysteine proteases known as *caspases* (42). It has been shown that mice lacking the death receptor Fas or mice treated with chemical inhibitors of caspases have reduced heart infarct sizes and fewer apoptosis-positive cells after ischemia-reperfusion injuries (43). In contrast to apoptosis, necroptosis, or programmed necrosis, causes severe inflammation and tissue damage during disease (44). Necroptosis is modulated by activation of RIP1, RIP3, and the effector molecule MLKL (25, 45). Recently, Yin and colleagues showed that a nonspecific inhibitor of RIP1, necrostatin-1, could reduce infarct sizes after major ischemia or reperfusion injuries (46). Using an NHP model, we showed that cardiomyocytes undergo RIP1-RIP3-MLKL–dependent necroptosis, and necroptosis inhibition with a selective drug has been shown to be protective against *S. pneumoniae*–induced cardiac damage, as reported by Gonzalez-Juarbe and colleagues (47). This finding is significant because killing cardiomyocytes and inducing a proinflammatory response may contribute to the generation of MACE during pneumococcal pneumonia.

Antibiotics have been shown to drastically reduce mortality resulting from pneumonia and other infectious diseases, and they are the cornerstone of CAP treatment (5). Thus, to mimic the disease evolution of CAP in humans, we treated NHPs with ampicillin to explore whether antibiotic treatment could prevent the development of cardiac injury secondary to *S. pneumoniae* invasion. We found that antibiotic treatment did not protect NHPs from the development of necroptosis or cardiac injury and, more important, that NHPs treated with antibiotics had scar formation in the heart. These findings are consistent with our findings in mice rescued from IPD with antibiotics (17) and of other experiments in mice with ischemia-reperfusion injury (31). This finding improves our understanding of MACE and the long-term mortality of patients with CAP. As described by Souders and colleagues, once cardiomyocytes die, heart tissue is replaced with myofibroblasts that produce an extracellular matrix that is rich in collagen and leads to scar formation (48). Because *S. pneumoniae* is capable of inducing cardiac scar formation, and because cardiac scars are known to cause

4C/FPO
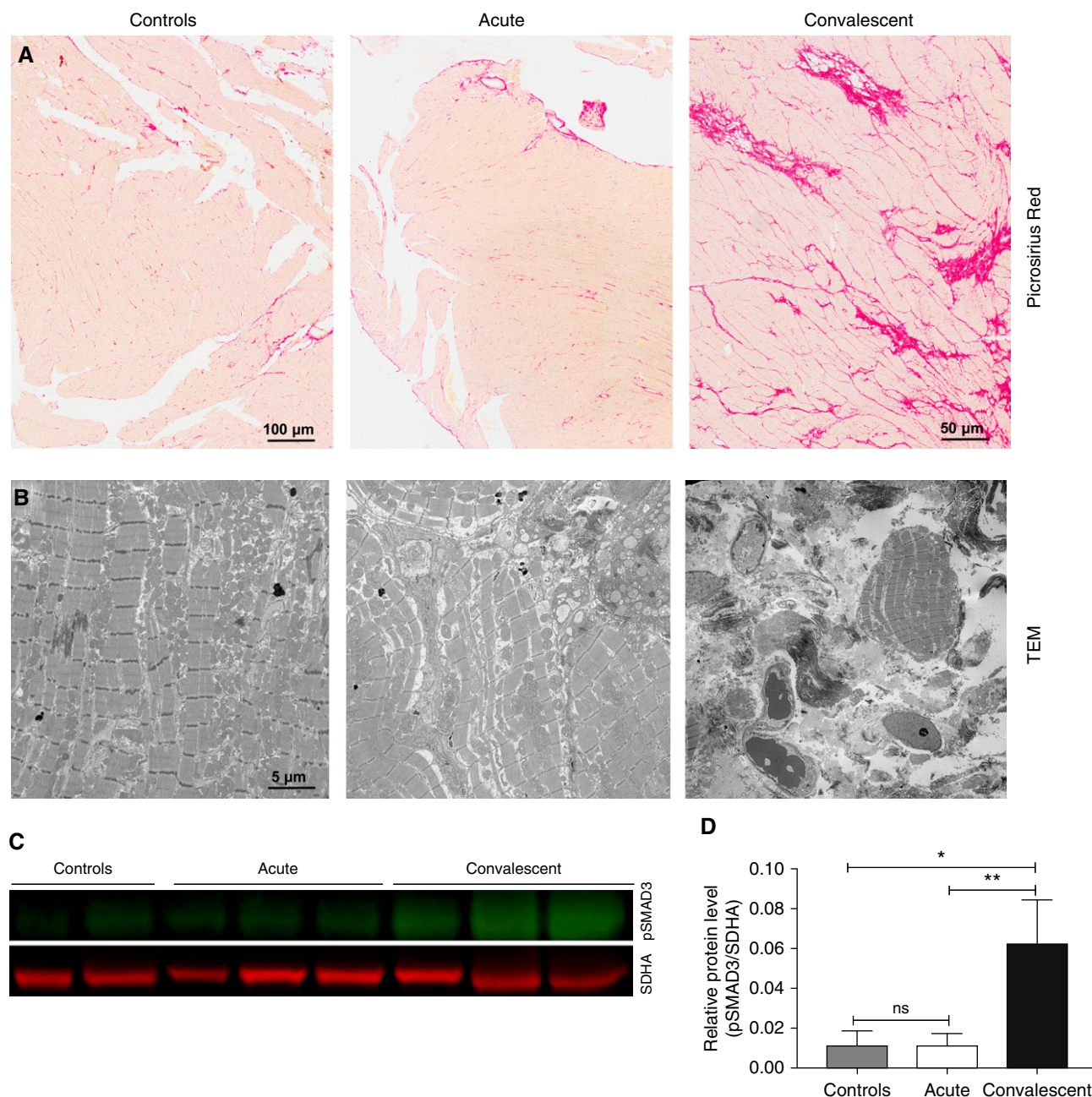
Figure 7. *Streptococcus pneumoniae* induces *de novo* collagen deposition in nonhuman primates (NHPs) with convalescent pneumonia. Representative images of heart sections from the six NHPs infected with *S. pneumoniae* and three uninfected control animals. (*A*) Picrosirius red was used to identify collagen deposition. NHPs with convalescent pneumonia developed collagen deposition throughout the left ventricle and interventricular septum. (*B*) Transmission electron microscopy (TEM) was used to confirm collagen deposition, identifying areas with conglomerates of collagen fibers in NHPs that survived their acute pneumonia. (*C*) The upregulation of pSMAD3 in convalescent NHPs was identified by immunoblot analysis, and (*D*) relative protein levels (pSMAD3/succinate dehydrogenase complex, subunit A [SDHA; loading control]) were determined using LI-COR Image Studio Lite software. Values are shown as medians and interquartile ranges. Unpaired nonparametric Mann-Whitney *U* tests were used to analyze statistical differences among the groups. *$*P < 0.05$; $**P < 0.01$; ns = not significant.

arrhythmias and heart failure, our findings might explain why MACE occur up to 10 years after the acute infection.

MACE are the result of a complex host–pathogen interaction between underlying comorbidities, the infectious pathogen (9), systemic inflammation (49), endothelial dysfunction (50), a relative prothrombotic state (9), increased cardiac oxygen demand, and low blood oxygen levels, which places considerable stress on the heart (9). In this study, we show that pathogen-specific mechanisms of *S. pneumoniae* contribute to the development of cardiac damage during

pneumococcal pneumonia that could lead to MACE.

Our study has some important limitations. First, the experimental design was limited to a 2-week maximum duration, and the findings should not be interpreted as long-term clinical outcomes after surviving CAP. Second, the clinical evaluation was limited in capabilities to continuously assess oxygenation or hemodynamic parameters that could be associated with cardiac injury. However, at the end of the experiments, the NHPs were not hypotensive to a level requiring vasopressor support. Third, we did not specifically examine coronary arteries to identify thrombi or signs of

myocardial infarction. However, we ruled out the clinical diagnosis of myocardial infarction according to the current guidelines of the American Heart Association (51). Finally, the sample size was limited to six NHPs with pneumococcal pneumonia owing to ethical considerations and high costs associated with the implantable continuous noninvasive cardiovascular monitoring systems and intensive veterinary medical care.

In summary, severe pneumococcal pneumonia led to the development of cardiac injury due to direct pathogen invasion, induction of cell death

(necroptosis and apoptosis), and subsequent cardiac scar formation after antibiotic treatment in an NHP model. Further research is needed to develop strategies to mitigate the pathological mechanisms underlying cardiac injury secondary to pneumococcal invasion. ∎

References

1. Wunderink RG, Waterer GW. Community-acquired pneumonia. *N Engl J Med* 2014;370:1863.
2. Prina E, Ranzani OT, Torres A. Community-acquired pneumonia. *Lancet* 2015;386:1097–1108.
3. GBD 2015 Mortality and Causes of Death Collaborators. Global, regional, and national life expectancy, all-cause mortality, and cause-specific mortality for 249 causes of death, 1980-2015: a systematic analysis for the Global Burden of Disease Study 2015. *Lancet* 2016; 388:1459–1544.
4. Torres A, Sibila O, Ferrer M, Polverino E, Menendez R, Mensa J, Gabarrús A, Sellarés J, Restrepo MI, Anzueto A, et al. Effect of corticosteroids on treatment failure among hospitalized patients with severe community-acquired pneumonia and high inflammatory response: a randomized clinical trial. *JAMA* 2015;313:677–686.
5. Musher DM, Thorner AR. Community-acquired pneumonia. *N Engl J Med* 2014;371:1619–1628.
6. Corrales-Medina VF, Alvarez KN, Weissfeld LA, Angus DC, Chirinos JA, Chang CC, Newman A, Loehr L, Folsom AR, Elkind MS, et al. Association between hospitalization for pneumonia and subsequent risk of cardiovascular disease. *JAMA* 2015;313:264–274.
7. Corrales-Medina VF, Taljaard M, Yende S, Kronmal R, Dwivedi G, Newman AB, Elkind MS, Lyles MF, Chirinos JA. Intermediate and long-term risk of new-onset heart failure after hospitalization for pneumonia in elderly adults. *Am Heart J* 2015;170:306–312.
8. Corrales-Medina VF, Taljaard M, Fine MJ, Dwivedi G, Perry JJ, Musher DM, Chirinos JA. Risk stratification for cardiac complications in patients hospitalized for community-acquired pneumonia. *Mayo Clin Proc* 2014;89:60–68.
9. Corrales-Medina VF, Musher DM, Shachkina S, Chirinos JA. Acute pneumonia and the cardiovascular system. *Lancet* 2013;381: 496–505.
10. Corrales-Medina VF, Musher DM, Wells GA, Chirinos JA, Chen L, Fine MJ. Cardiac complications in patients with community-acquired pneumonia: incidence, timing, risk factors, and association with short-term mortality. *Circulation* 2012;125:773–781.
11. Viasus D, Garcia-Vidal C, Manresa F, Dorca J, Gudiol F, Carratalà J. Risk stratification and prognosis of acute cardiac events in hospitalized adults with community-acquired pneumonia. *J Infect* 2013;66:27–33.
12. Musher DM, Rueda AM, Kaka AS, Mapara SM. The association between pneumococcal pneumonia and acute cardiac events. *Clin Infect Dis* 2007;45:158–165.
13. Corrales-Medina VF, Suh KN, Rose G, Chirinos JA, Doucette S, Cameron DW, Fergusson DA. Cardiac complications in patients with community-acquired pneumonia: a systematic review and meta-analysis of observational studies. *PLoS Med* 2011;8:e1001048.
14. Jain S, Self WH, Wunderink RG, Fakhran S, Balk R, Bramley AM, Reed C, Grijalva CG, Anderson EJ, Courtney DM, et al.; CDC EPIC Study Team. Community-acquired pneumonia requiring hospitalization among U.S. adults. *N Engl J Med* 2015;373:415–427.
15. Aliberti S, Reyes LF, Faverio P, Sotgiu G, Dore S, Rodriguez AH, Soni NJ, Restrepo MI; GLIMP investigators. Global Initiative for Methicillin-resistant *Staphylococcus aureus* Pneumonia (GLIMP): an international, observational cohort study. *Lancet Infect Dis* 2016;16:1364–1376.
16. Rae N, Finch S, Chalmers JD. Cardiovascular disease as a complication of community-acquired pneumonia. *Curr Opin Pulm Med* 2016;22:212–218.
17. Brown AO, Mann B, Gao G, Hankins JS, Humann J, Giardina J, Faverio P, Restrepo MI, Halade GV, Mortensen EM, et al. *Streptococcus pneumoniae* translocates into the myocardium and forms unique microlesions that disrupt cardiac function. *PLoS Pathog* 2014;10:e1004383.
18. Gilley RP, González-Juarbe N, Shenoy AT, Reyes LF, Dube PH, Restrepo MI, Orihuela CJ. Infiltrated macrophages die of pneumolysin-mediated necroptosis following pneumococcal myocardial invasion. *Infect Immun* 2016;84:1457–1469.
19. Alhamdi Y, Neill DR, Abrams ST, Malak HA, Yahya R, Barrett-Jolley R, Wang G, Kadioglu A, Toh CH. Circulating pneumolysin is a potent inducer of cardiac injury during pneumococcal infection. *PLoS Pathog* 2015;11:e1004836.
20. Fillon S, Soulis K, Rajasekaran S, Benedict-Hamilton H, Radin JN, Orihuela CJ, El Kasmi KC, Murti G, Kaushal D, Gaber MW, et al. Platelet-activating factor receptor and innate immunity: uptake of gram-positive bacterial cell wall into host cells and cell-specific pathophysiology. *J Immunol* 2006;177:6182–6191.
21. Feldman C, Anderson R. Recent advances in our understanding of *Streptococcus pneumoniae* infection. *F1000Prime Rep* 2014;6:82.
22. Brown AO, Millett ER, Quint JK, Orihuela CJ. Cardiotoxicity during invasive pneumococcal disease. *Am J Respir Crit Care Med* 2015; 191:739–745.
23. González-Juarbe N, Gilley RP, Hinojosa CA, Bradley KM, Kamei A, Gao G, Dube PH, Bergman MA, Orihuela CJ. Pore-forming toxins induce macrophage necroptosis during acute bacterial pneumonia. *PLoS Pathog* 2015;11:e1005337.
24. Zhang T, Zhang Y, Cui M, Jin L, Wang Y, Lv F, Liu Y, Zheng W, Shang H, Zhang J, et al. CaMKII is a RIP3 substrate mediating ischemia- and oxidative stress-induced myocardial necroptosis. *Nat Med* 2016;22:175–182.
25. Linkermann A, Hackl MJ, Kunzendorf U, Walczak H, Krautwald S, Jevnikar AM. Necroptosis in immunity and ischemia-reperfusion injury. *Am J Transplant* 2013;13:2797–2804.
26. Linkermann A, Bräsen JH, Darding M, Jin MK, Sanz AB, Heller JO, De Zen F, Weinlich R, Ortiz A, Walczak H, et al. Two independent pathways of regulated necrosis mediate ischemia-reperfusion injury. *Proc Natl Acad Sci USA* 2013;110:12024–12029.

27. Restrepo MI, Reyes LF, Anzueto A. Complication of community-acquired pneumonia (including cardiac complications). *Semin Respir Crit Care Med* 2016;37:897–904.

28. Reyes LF, Restrepo MI, Hinojosa CA, Soni NJ, Shenoy AT, Gilley RP, Gonzalez-Juarbe N, Noda JR, Winter VT, de la Garza MA, *et al*. A non-human primate model of severe pneumococcal pneumonia. *PLoS One* 2016;11:e0166092.

29. Tettelin H, Nelson KE, Paulsen IT, Eisen JA, Read TD, Peterson S, Heidelberg J, DeBoy RT, Haft DH, Dodson RJ, *et al*. Complete genome sequence of a virulent isolate of *Streptococcus pneumoniae*. *Science* 2001;293:498–506.

30. Giavedoni LD. Simultaneous detection of multiple cytokines and chemokines from nonhuman primates using Luminex technology. *J Immunol Methods* 2005;301:89–101.

31. Bujak M, Frangogiannis NG. The role of TGF-β signaling in myocardial infarction and cardiac remodeling. *Cardiovasc Res* 2007;74:184–195.

32. Paizis G, Gilbert RE, Cooper ME, Murthi P, Schembri JM, Wu LL, Rumble JR, Kelly DJ, Tikellis C, Cox A, *et al*. Effect of angiotensin II type 1 receptor blockade on experimental hepatic fibrogenesis. *J Hepatol* 2001;35:376–385.

33. Goldsmith EC, Bradshaw AD, Spinale FG. Cellular mechanisms of tissue fibrosis. 2. Contributory pathways leading to myocardial fibrosis: moving beyond collagen expression. *Am J Physiol Cell Physiol* 2013;304:C393–C402.

34. Kim JH, Park MY, Kim CN, Kim KH, Kang HB, Kim KD, Kim JW. Expression of endothelial cell-specific molecule-1 regulated by hypoxia inducible factor-1α in human colon carcinoma: impact of ESM-1 on prognosis and its correlation with clinicopathological features. *Oncol Rep* 2012;28:1701–1708.

35. Restrepo MI, Mortensen EM, Rello J, Brody J, Anzueto A. Late admission to the ICU in patients with community-acquired pneumonia is associated with higher mortality. *Chest* 2010;137: 552–557.

36. Mandell LA, Wunderink RG, Anzueto A, Bartlett JG, Campbell GD, Dean NC, Dowell SF, File TM Jr, Musher DM, Niederman MS, *et al*.; Infectious Diseases Society of America; American Thoracic Society. Infectious Diseases Society of America/American Thoracic Society consensus guidelines on the management of community-acquired pneumonia in adults. *Nephrol Dial Transplant* 2007;44(Suppl 2): S27–S72.

37. Rudiger A, Singer M. The heart in sepsis: from basic mechanisms to clinical management. *Curr Vasc Pharmacol* 2013;11:187–195.

38. Zaky A, Gill EA, Lin CP, Paul CP, Bendjelid K, Treggiari MM. Characteristics of sepsis-induced cardiac dysfunction using speckle-tracking echocardiography: a feasibility study. *Anaesth Intensive Care* 2016;44:65–76.

39. Ammann P, Fehr T, Minder EI, Günter C, Bertel O. Elevation of troponin I in sepsis and septic shock. *Intensive Care Med* 2001;27:965–969.

40. Altmann DR, Korte W, Maeder MT, Fehr T, Haager P, Rickli H, Kleger GR, Rodriguez R, Ammann P. Elevated cardiac troponin I in sepsis and septic shock: no evidence for thrombus associated myocardial necrosis. *PLoS One* 2010;5:e9017.

41. Vestjens SMT, Spoorenberg SMC, Rijkers GT, Grutters JC, Ten Berg JM, Noordzij PG, Van de Garde EMW, Bos WJW; Ovidius Study Group. High-sensitivity cardiac troponin T predicts mortality after hospitalization for community-acquired pneumonia. *Respirology* 2017;22:1000–1006.

42. Chiong M, Wang ZV, Pedrozo Z, Cao DJ, Troncoso R, Ibacache M, Criollo A, Nemchenko A, Hill JA, Lavandero S. Cardiomyocyte death: mechanisms and translational implications. *Cell Death Dis* 2011;2:e244.

43. Lee P, Sata M, Lefer DJ, Factor SM, Walsh K, Kitsis RN. Fas pathway is a critical mediator of cardiac myocyte death and MI during ischemia-reperfusion in vivo. *Am J Physiol Heart Circ Physiol* 2003;284: H456–H463.

44. Pasparakis M, Vandenabeele P. Necroptosis and its role in inflammation. *Nature* 2015;517:311–320.

45. Silke J, Rickard JA, Gerlic M. The diverse role of RIP kinases in necroptosis and inflammation. *Nat Immunol* 2015;16:689–697.

46. Yin B, Xu Y, Wei RL, He F, Luo BY, Wang JY. Inhibition of receptor-interacting protein 3 upregulation and nuclear translocation involved in necrostatin-1 protection against hippocampal neuronal programmed necrosis induced by ischemia/reperfusion injury. *Brain Res* 2015;1609:63–71.

47. Gonzalez-Juarbe N, Gilley R, Riegler AN, Bradley KM, Reyes LF, Shenoy AT, Brissac T, Herrera AI, Dube PH, Restrepo MI, *et al*. Necroptosis: a major cell death mechanism induced by pore-forming toxins during bacterial pneumonia. Presented at the Institutional Research and Academic Career Development Award Annual Meeting. June 5, 2017, Birmingham, AL. Abstract E69, p. 23.

48. Souders CA, Bowers SL, Baudino TA. Cardiac fibroblast: the renaissance cell. *Circ Res* 2009;105:1164–1176.

49. Mann DL. Inflammatory mediators and the failing heart: past, present, and the foreseeable future. *Circ Res* 2002;91:988–998.

50. Aliberti S, Ramirez JA. Cardiac diseases complicating community-acquired pneumonia. *Curr Opin Infect Dis* 2014;27:295–301.

51. Amsterdam EA, Wenger NK, Brindis RG, Casey DE Jr, Ganiats TG, Holmes DR Jr, Jaffe AS, Jneid H, Kelly RF, Kontos MC, *et al*.; American College of Cardiology; American Heart Association Task Force on Practice Guidelines; Society for Cardiovascular Angiography and Interventions; Society of Thoracic Surgeons; American Association for Clinical Chemistry. 2014 AHA/ACC Guideline for the Management of Patients with Non-ST-Elevation Acute Coronary Syndromes: a report of the American College of Cardiology/American Heart Association Task Force on Practice Guidelines. *J Am Coll Cardiol* 2014;64:e139–e228.